



An investigation of the vibration of multi-layer composite beams reinforced by graphene platelets resting on two parameter viscoelastic foundation

Saeedeh Qaderi¹ · Farzad Ebrahimi¹  · Ali Seyfi¹

© Springer Nature Switzerland AG 2019

Abstract

The current study goal is to analyze free vibration behavior of multi-layer composite beams reinforced by graphene platelets resting on viscoelastic foundation. These material properties varies layer to layer in the thickness direction. GPLs are spreaded in each layer randomly and four different distribution patterns are employed and all parameter effects on these four are investigated. Effective material properties are estimated by Halpin–Tsai model and higher order shear deformation beam theory is utilized to achieve the theoretical formulation of multi-layer GPLRC beam and Navier solution have been used to derive and follow up the governing differential equation of motion and natural frequency. To find out the effect of GPLs on composite structures and effect of different distribution pattern of GPLs on frequency of the beam structure and the other parameters, all sections of this study and results are presented based on four GPLs distribution patterns.

Keywords Dynamic analysis · Vibration · Multi-layer · Graphene platelet—reinforced composite beams · Viscoelastic foundation

1 Introduction

Recent researches insisted on applications of different composites in different engineering fields including civil engineering, aerospace, biomedical, and automotive. Also due to recent advancement in science and technology, carbon nanofillers as an important reinforcement in composite structures have shown great potential in constructional engineering due to their preferable mechanical properties [3, 10, 11]; in comparison with carbon nanofillers, graphene or graphene platelets (GPLs) as a reinforcement for composites, have low production cost with high specific surface areas up to $2630 \text{ m}^2 \text{ g}^{-2}$ [2, 7, 24, 25, 30]; graphene platelets with tensile strength of 130 GPA is an appropriate candidate as a reinforcement in composite materials [2, 7, 24, 25, 30]; the other point that convinced researchers to use fillers in composite structures is that

subjoining even a poor amount of graphene or other fillers to base material can improve its properties as thermal properties, mechanical properties and electrical too [18, 20, 23–25]; so, logically a large part of sections in this project have been allocated to the improvement of material properties with adding even a low amount of GPLs. In order to validate the claim that GPLs improve mechanical properties of composites [19] determined that 0.1% additional (wt%) GPLs in polymer composites improved the different properties of composites such as strength and stiffness. Also Wang et al. [29] achieved that Young's modulus of epoxy reinforced nanocomposites increases approximately 0.64 GPA by adding 6.0 wt% of GPLs as fillers in the composite plate. Comparing graphene and carbon nanotubes as filler and reinforcement for composite, results showed that graphene has a superior point than Carbon nanotubes (CNTs), such as significant stiffness, supreme

✉ Farzad Ebrahimi, febrahimi@eng.ikiu.ac.ir | ¹Department of Mechanics, Faculty of Engineering, Imam Khomeini International University, Qazvin 3414916818, Iran.



strength but low mass density [15]; recently, nanocomposites that reinforced with graphene and its formatives become a widespread topic of researchers; also alumina ceramic composites reinforced with GPLs is studied by Liu et al. [17] and they found that mechanical properties of this composites have been improved too. Ji et al. [12] have been studied the graphene reinforced composites and have been used the Mori–Tanaka model to calculate the effective elastic properties. FEM (finite element method) as a multiscale method have been used by Spanos et al. [28] to achieve atomistic molecular structural mechanics of composites reinforced with graphene. Ji et al. [12] studied the stiffening effect of graphene sheets on polymer nanocomposites and they found that embedding even a low amount of sheets of graphene can extremely increase the effective stiffness of the epoxy matrix. Finite element method is employed to analyze the vibration behavior of composite beams reinforced with graphene platelets (GPLs) [6]; functionally graded carbon nanotube reinforced composite beams with geometric imperfections have been studied by Wu et al. [31]; Thermal buckling analysis of carbon nanotube reinforced composite beams has done too and all important derivatives of structure properties and CNTs effect on composite beams are presented [21, 22]; studying the dynamic behavior of structures based on carbon is used widely in mechanical engineering, recently. Also linear and nonlinear free and forced vibration, bending, elastic buckling, post buckling of composite structures reinforced CNTs have been widely probed [1, 13, 14, 21, 22, 31].

Natural frequencies of polymer composites reinforced graphene have been presented by Chandra et al. [5] using finite element method. Feng et al. [8, 9] also published an article through the nonlinear vibration of multi-layer nanocomposite beam based on Timoshenko beam theory and Von Karman strain–displacement relationship and presented. Bending analysis of polymer nanocomposite beams reinforced with graphene platelets have been studied by Feng et al. [8, 9] and Ritz method employed to reduce the governing differential equation into an algebraic system.

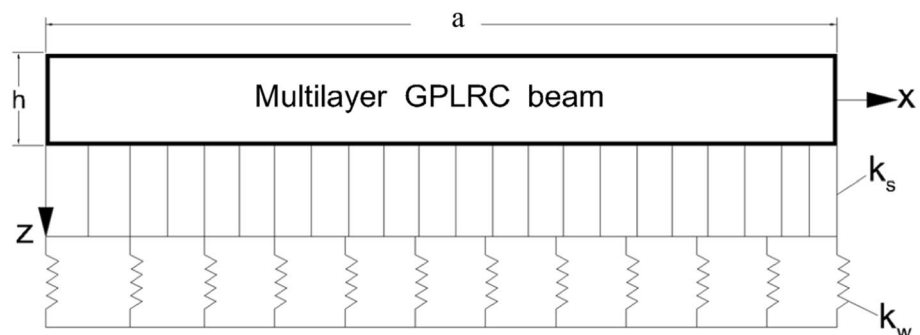
Barati and Zenkour [4] also studied post-buckling behavior of shear deformable graphene platelet reinforced beams with porosities. Kitipornchai et al. [16] presented a project on free vibration and elastic buckling of functionally graded porous beams reinforced by graphene platelets and resulted that graphene platelets are considered as ideal material for composite reinforcements and improved mechanical properties of composite structures. Shabanlou et al. [26] used finite element method to study free vibration behavior of multi-layer composite beams reinforced GPLs.

No work has been done at vibration analysis of multi-layer GPLRC beams resting on viscoelastic foundation using higher order shear deformation beam theory whereas non-uniformly distributed different GPL patterns are considered. Recent researches focused on the nanocomposites construction and their material properties but present study has been analyzed the vibrational behavior of multi-layer GPLRC beam resting on two parameter viscoelastic foundation considering effects of four different distribution patterns on mechanical parameters of GPLRC beams in detail.

2 Problem formulation

As shown in Fig. 1 four different types of GPLs distribution of multi-layer polymer composite beam with h as thickness dimension and a as length of the beam is considered. N_l is defined the number of layers of GPLRC beam with equal amount of thickness for every layer of the beam structure ($\Delta h = \frac{h}{N}$). To form a functionally graded structure, the GPLs weight fraction is varied layer to layer based on Eqs. (1)–(4). As shown in Fig. 2 four different distribution pattern are considered which pattern 1 is an isotropic homogeneous beam case that GPLs (wt% of GPLs 1%) are regularly distributed at every individual layer. Pattern 2 presented GPL weight fraction (wt%) changes layer to layer along the thickness, as shown in Fig. 2. In the other words, GPLs weight fraction is the highest in the mid-plane

Fig. 1 Multi-layer GPLRC beam resting on elastic foundation



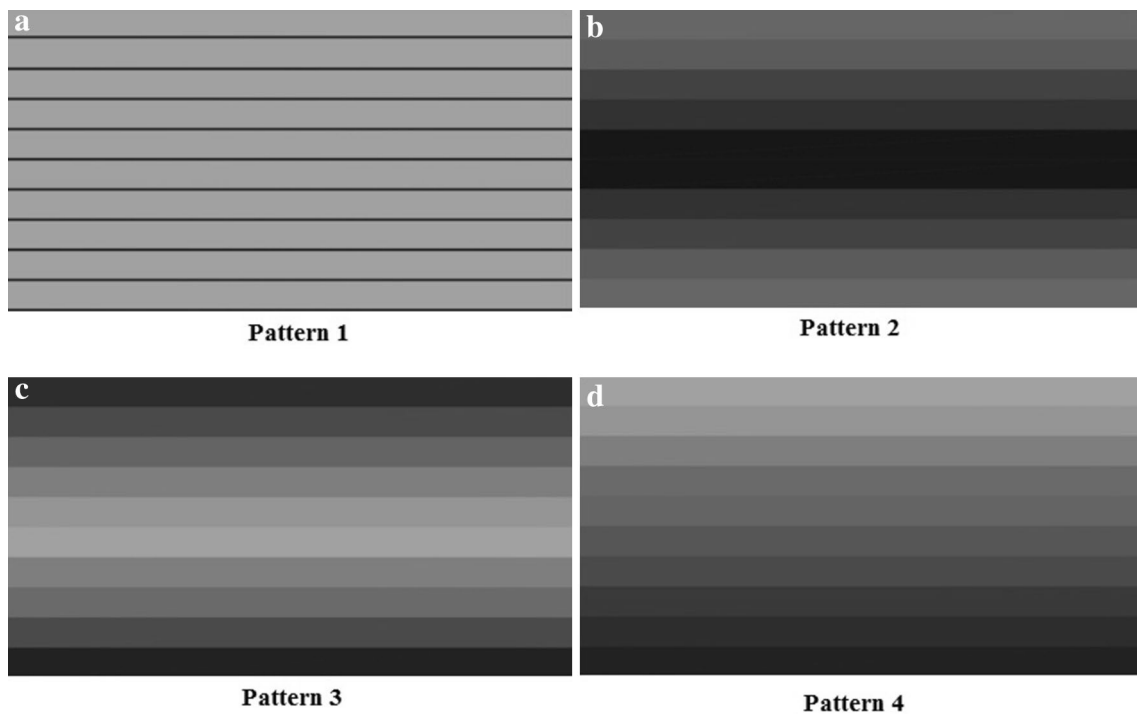


Fig. 2 **a** Homogeneous distribution, **b** GPL distribution based on pattern 2, **c** GPL distribution based on pattern 3, **d** different GPL distribution pattern

and is decreased layer to layer when it moves to the top and bottom layer in pattern 2. In contrast to pattern 2, in pattern 3 both top and bottom layers are consisting the maximum weight fraction of GPLs and changes to the lowest by moving to the mid-plane while pattern 4 is non-symmetrical pattern and linear increasing is shown in Fig. 2 for GPLs weight fraction from top to the bottom surface.

The volume fraction functions of these four GPL distribution pattern have been represented as [27]:

Pattern 1 : $V_{GPL}(k) = V_{GPL}^*$ (1)

Pattern 2 : $V_{GPL} = 2V_{GPL}^* |2k - N_L - 1| / N_L$, (2)

Pattern 3 : $V_{GPL} = 2V_{GPL}^* (1 - |2k - N_L - 1| / N_L)$ (3)

Pattern 4 : $V_{GPL} = 2V_{GPL}^* (2k - 1) / N_L$ (4)

where k is number of GPLRC beam layers, $k = 1, 2, \dots, N_L$ and V_{GPL}^* is the total volume fraction of GPLs.

3 Effective material properties

Based on Halpin–Tsai model, the effective elastic modulus of GPLRC approximated by [27]:

$$E = \frac{3}{8}E_L + \frac{5}{8}E_T \tag{5}$$

where E is effective modulus of GPLRC and E_L is the longitudinal modulus for unidirectional laminate calculated by the Halpin–Tsai model and E_T is the transverse modulus of laminate.

$$E_L = \frac{1 + \xi_L \eta_L V_{GPL}}{1 - \eta_L V_{GPL}} \times E_m \tag{6}$$

$$E_T = \frac{1 + \xi_t \eta_T V_f}{1 - \eta_T V_f} \times E_m \tag{7}$$

where

$$\xi_L = 2(l_{GPL} / h_{GPL}) \tag{8}$$

$$\xi_t = 2(w_{GPL} / h_{GPL}) \tag{9}$$

where l_{GPL} , h_{GPL} , w_{GPL} are GPLs dimensions.

$$\text{And } \eta_L = \frac{\left(\frac{E_{GPL}}{E_M}\right) - 1}{\left(\frac{E_{GPL}}{E_M}\right) + \xi_L} \tag{10}$$

$$\eta_T = \frac{\left(\frac{E_{GPL}}{E_M}\right) - 1}{\left(\frac{E_{GPL}}{E_M}\right) + \xi_t} \tag{11}$$

By using rule of mixture, Mass density ρ_c and Possion's ratio ν_c of the GPL/nanocomposite is presented as [27]:

$$\rho_c = \rho_{GPL}V_{GPL} + \rho_MV_M \tag{12}$$

$$\nu_c = \nu_{GPL}V_{GPL} + \nu_MV_M \tag{13}$$

where V_M is the volume fraction of epoxy matrix.

The governing equation of V_{GPL}^* is:

$$V_{GPL}^* = \frac{W_{GPL}}{W_{GPL} + (\rho_{GPL}/\rho_m)(1 - W_{GPL})} \tag{14}$$

where W_{GPL} is GPL weight fraction; ρ_{GPL} and ρ_m are the mass densities of GPLs and the epoxy matrix.

4 Governing equation

Based on the higher-order shear deformation theory the displacement of beam along x, y and z direction are represented as:

$$u(x, z, t) = u_0(x, t) + z\phi_x(x, t) - c_1z^3 \left[\phi_x(x, t) + \frac{\partial w_0(x, t)}{\partial x} \right] \tag{15}$$

$$v(x, z, t) = 0$$

$$w(x, z, t) = w_0(x, t)$$

where c_1 is equal to $4/3h^2$ and where u and v are the in-plane displacements at anypoint (x, y, z) and u_0 define the in-plane displacement of the point (x, y, 0) on the mid-plane, w is the deflection, and ϕ_x is the rotation of the normals to the mid-plane about x axes.

From the linear elastic stress–strain constitutive relationship, the stress matrix of the multi-layer GPLRC beam is presented as:

$$\begin{Bmatrix} \sigma_{xx} \\ \sigma_{yy} \\ \sigma_{xy} \\ \sigma_{xz} \\ \sigma_{yz} \end{Bmatrix} = \begin{Bmatrix} Q_{11} & Q_{12} & 0 & 0 & 0 \\ Q_{21} & Q_{22} & 0 & 0 & 0 \\ 0 & 0 & Q_{44} & 0 & 0 \\ 0 & 0 & 0 & Q_{55} & 0 \\ 0 & 0 & 0 & 0 & Q_{66} \end{Bmatrix} \begin{Bmatrix} \epsilon_{xx} \\ \epsilon_{yy} \\ \gamma_{xy} \\ \gamma_{xz} \\ \gamma_{yz} \end{Bmatrix} \tag{16}$$

Based on Hamilton principal:

$$\int_{t_1}^{t_2} (\delta T - \delta U + \delta W_2 - \delta D) dt = 0 \tag{17}$$

Work done by viscoelastic foundation is:

$$\delta W_2 = \int_0^L \left\{ -K_w w + K_p \frac{\partial^2 w}{\partial x^2} \right\} \delta w dx \tag{18}$$

where K_p and K_w are Pasternak and Winkler coefficient.

External work done by damper is presented as:

$$\delta D = \iint_A \left\{ C_d \frac{\partial w_0}{\partial t} \frac{\partial}{\partial t} \delta w_0 \right\} dA \tag{19}$$

Finally governing equation of GPLRC with the effect of viscoelastic foundation resulted in:

$$\begin{aligned} \delta u_0 : \frac{\partial N_{xx}}{\partial x} &= I_0 \frac{\partial^2 u_0}{\partial t^2} + I_1 \frac{\partial^2 \phi_x}{\partial t^2} - I_3 c_1 \left(\frac{\partial^2 \phi_x}{\partial t^2} + \frac{\partial^3 w_0}{\partial t^2 \partial x} \right), \\ \delta w_0 : c_1 \frac{\partial^2 P_{xx}}{\partial x^2} + \frac{\partial Q_{xz}}{\partial x} - 3c_1 \frac{\partial S_{xz}}{\partial x} &+ K_w w_0 + K_p \left(\frac{\partial^2 w_0}{\partial x^2} \right) + C_d \left(\frac{\partial w_0}{\partial t} \right) \\ &= c_1 I_3 \frac{\partial^3 u_0}{\partial x \partial t^2} + c_1 I_4 \frac{\partial^3 \phi_x}{\partial x \partial t^2} - I_6 c_1^2 \left(\frac{\partial^3 \phi_x}{\partial x \partial t^2} + \frac{\partial^4 w_0}{\partial t^2 \partial x^2} \right) \\ &+ \left(I_0 \frac{\partial^2 w_0}{\partial t^2} \right) + K_w w_0 + K_p \left(\frac{\partial^2 w_0}{\partial x^2} \right) + C_d \left(\frac{\partial w_0}{\partial t} \right) \\ \delta \phi_x : \frac{\partial M_{xx}}{\partial x} - c_1 \frac{\partial P_{xx}}{\partial x} - Q_{xz} + 3c_1 S_{xz} &= I_1 \frac{\partial^2 u_0}{\partial t^2} + I_2 \frac{\partial^2 \phi_x}{\partial t^2} \\ &- I_4 c_1 \left(\frac{\partial^2 \phi_x}{\partial t^2} + \frac{\partial^3 w_0}{\partial t^2 \partial x} \right) \\ &- c_1 I_3 \frac{\partial^2 u_0}{\partial t^2} - c_1 I_4 \frac{\partial^2 \phi_x}{\partial t^2} + I_6 c_1^2 \left(\frac{\partial^2 \phi_x}{\partial t^2} + \frac{\partial^3 w_0}{\partial t^2 \partial x} \right) \end{aligned} \tag{20}$$

where parameters used in the above equation are defined as:

$$\{I_0, I_1, I_2, I_3, I_4, I_5, I_6\} = \sum_{k=1}^{N_l} \int_{z_k}^{z_{k+1}} \rho^k \{1, z, z^2, z^3, z^4, z^5, z^6\} dz$$

where ρ^k is the mass density of kth layer of GPLRC beam.

5 Solution procedure

Navier solution is used to continue solution procedure:

$$\begin{Bmatrix} u(x, y, z) \\ w(x, y, z) \\ \phi_x(x, y, z) \end{Bmatrix} = \sum_{m=1}^{\infty} \sum_{n=1}^{\infty} \begin{Bmatrix} U_{mn} \cos \frac{m\pi x}{a} e^{iwt} \\ W_{mn} \sin \frac{m\pi x}{a} e^{iwt} \\ X_{mn} \cos \frac{m\pi x}{a} e^{iwt} \end{Bmatrix} \tag{21}$$

where U_{mn} , W_{mn} and X_{mn} are dimensionless functions of time and m and n are defined as mode number of vibration of GPLRC beam.

The boundary condition equation of simply supported beam in all edges can be written as:

$$S - S \text{ at } x = 0, a \rightarrow W = 0, \quad N_{xx} = M_{xx} = 0 \quad (22)$$

So matrixes resulted by solving governing equations based on Navier solution are:

$$\begin{bmatrix} K_{11} & K_{12} & K_{13} \\ K_{21} & K_{22} & K_{23} \\ K_{31} & K_{32} & K_{33} \end{bmatrix} - \omega^2 \begin{bmatrix} M_{11} & M_{12} & M_{13} \\ M_{21} & M_{22} & M_{23} \\ M_{31} & M_{32} & M_{33} \end{bmatrix} \begin{bmatrix} u \\ w \\ \psi_x \end{bmatrix} + \omega \begin{bmatrix} C_{11} & C_{12} & C_{13} \\ C_{21} & C_{22} & C_{23} \\ C_{31} & C_{32} & C_{33} \end{bmatrix} = 0 \quad (23)$$

$$\begin{aligned} K_{11} &= -m^2 A_{11} - n^2 (A_{44}) \\ K_{12} &= c_1 m^3 (D_{11}) + c_1 n^2 m (D_{12}) + 2c_1 m n^2 (D_{44}) \\ K_{13} &= m^2 (B_{11}) + c_1 m^2 (D_{11}) + c_1 n^2 (D_{44}) - n^2 B_{44} \\ K_{21} &= K_{12} \\ K_{22} &= -c_1^2 m^4 (G_{12}) - 2c_1^2 m^2 n^2 (G_{12}) - 4c_1^2 (G_{44}) \\ &\quad - c_1^2 n^4 (G_{22}) - m^2 (A_{55} - 6c_1 C_{55} + 9c_1^2 E_{55}) \\ &\quad - n^2 (A_{66} - 3c_1 C_{66} + 9c_1^2 E_{66}) \\ K_{23} &= c_1 m^3 E_{11} - c_1^2 m^3 G_{11} \quad (24) \\ &\quad + m n^2 (c_1 E_{12} - c_1^2 G_{12} + 2c_1 E_{44} - 2c_1^2 G_{44}) \\ &\quad - 3c_1 m A_{55} C_{55} + 3c_1 m (C_{55} - 3c_1 E_{55}) \\ K_{31} &= K_{13} \\ K_{32} &= K_{23} \\ K_{33} &= -m^2 (c_1^2 G_{11} - 2c_1 E_{11} + C_{11}) \\ &\quad - n^2 (C_{44} - 2c_1 E_{44} + c_1^2 G_{44}) \\ &\quad + 3c_1 (C_{55} - 3c_1 E_{55}) - 3c_1 C_{55} A_{55} \end{aligned}$$

$$\begin{aligned} M_{11} &= -I_0 \\ M_{12} &= c_1 m I_3 \\ M_{13} &= -I_1 + c_1 I_3 \\ M_{21} &= c_1 m I_3 \\ M_{22} &= -I_0 - 2c_1^2 I_6 (m^2 + n^2) \quad (25) \\ M_{23} &= m c_1 I_4 - m c_1^2 I_6 \\ M_{31} &= M_{13} \\ M_{32} &= M_{23} \\ M_{33} &= -I_2 + 2c_1 I_4 - c_1^2 I_6 \end{aligned}$$

$$C_{11} = C_{12} = C_{13} = C_{21} = C_{23} = C_{31} = C_{32} = C_{33} \\ C_{22} = C_d$$

By setting the determinate of above matrixes equal to zero, answers are leded us to the vibration analysis of GPLRC beam.

6 Results and discussion

A complete research is done at multi-layer polymer beam reinforced by graphene platelets resting on viscoelastic foundation in the present study. The material properties of the matrix are given as:

$$l_{GPL} = 2.5 \mu m, \quad w_{GPL} = 1.5 \mu m, \quad h_{GPL} = 1.5 \mu m$$

Non-dimensional natural frequency of multi-layer GPLRC beam is given as follow:

$$\lambda = \omega h \sqrt{\rho_M / E_M} \quad (26)$$

The material properties of the GPL as a reinforcement and epoxy are given in Table 1:

6.1 Effects of elastic foundation on dimensionless frequency parameter (λ)

Variation of Winkler and Pasternak foundations coefficient is presented in this part and vibration behavior of GPLRC beam is studied in detail. Also all four GPLs distribution patterns and polymer matrix without any reinforcement are determined and the point is that in all patterns by increasing elastic coefficient (K_w and K_p), dimensionless frequency of the beam structure is shincreasing as shown in Figs. 3, 4, 5, 6 and 7. In Fig. 3 beam is studying without any reinforcement and by increasing Winkler factor to 3 N/m, dimensionless natural frequency presented an increasing process but when Winkler factor overpassed 3 N/m, the frequency is leded to constant amount and is continued to the end. By adding GPLs to the structure and studying the effects of Pasternak factor on vibration analysis of GPLRC beam, results showed that dimensionless frequency of the structure is increasing by Pasternak factor increasing.

It is clear that results derived, insisted on increasing process of dimensionless frequency of the structure by Winkler and Pasternak coefficient increasing in all four distribution pattern. Figure 4 presented variational diagram of pattern 1 which homogeneous distribution is governed. By two parameter elastic foundation increasing, frequency amount is started from 0.28 and leded to 0.3.

Comparing Figs. 3 and 4 have shown difference between layer-wise distribution and uniform distribution.

Table 1 Material properties of epoxy and GPL

Material properties	Polymer	GPL
Young's modulus (GPa)	3	1010
Poission's ratio	0.34	0.186
Density (kg m ⁻³)	1200	1062.5

Fig. 3 Elastic foundation effects on frequency of polymer beam

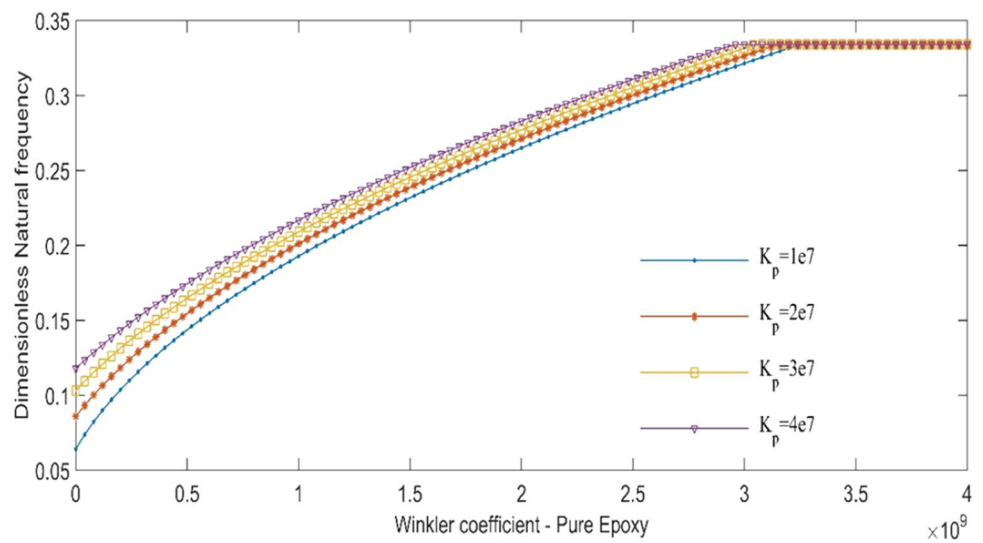
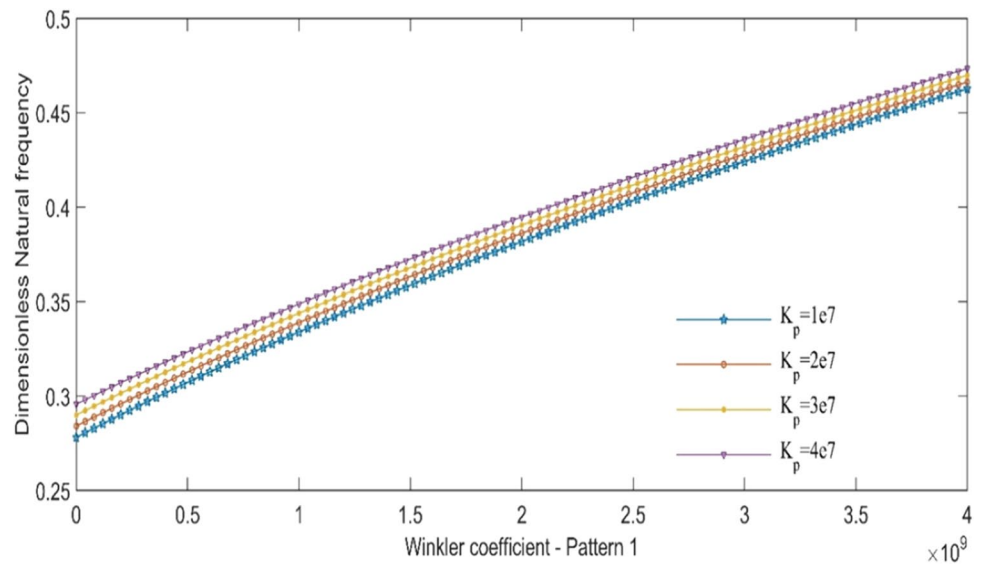


Fig. 4 Elastic foundation effects on frequency of GPLRC beam (pattern 1)



Frequency of GPLRC beam is started increasing process from smaller amount but is continued like pattern 1.

Pattern 3 and 4 also are presented increasing diagram of dimensionless frequency. In pattern 3 where more GPLs weight fraction spread out in outer layers, increasing process for dimensionless frequency is started from more numerical amount. Comparing pattern 3 and 4, multi-layer GPLRC beam resting on elastic foundation, these two patterns have shown increasing diagram but in Pattern 4 where GPL weight fraction changes layer to layer as moving to upper layers, increasing process is started from smaller amount.

6.2 Effects of damper on natural frequency of multi-layer GPLRC beam

In this section, studying the effects of elastic foundation on the vibrational behavior of the structure has done and K_w and K_p as Winkler coefficient and Pasternak coefficient and C_d as damper coefficient are determined. All four GPL distribution patterns are considered to analyze the vibrational parameters of the structure accurately. Based on Table 2 an increasing procedure for the natural frequency of beam is derived by increasing the amount of K_w and K_p . Also, results insisted on bigger amount of natural frequency for pattern 1 which GPLs are spreading homogeneous in all layers and the weight fraction of this nanofillers are same at all layers of beam than pattern 2 which the amount of GPLs weight fraction are changing linearly

Fig. 5 Elastic foundation effects on frequency of GPLRC beam (pattern 2)

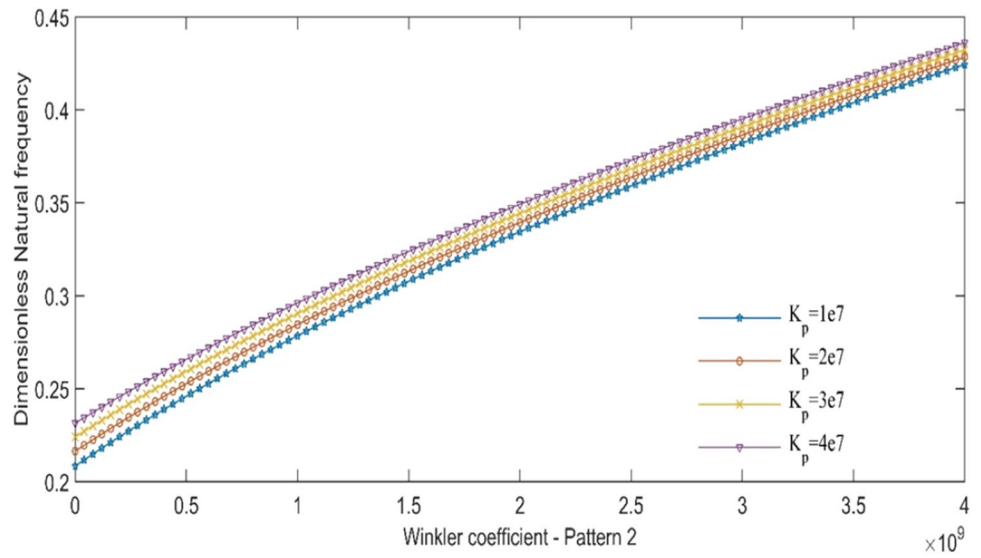


Fig. 6 Elastic foundation effects on frequency of GPLRC beam (pattern 3)

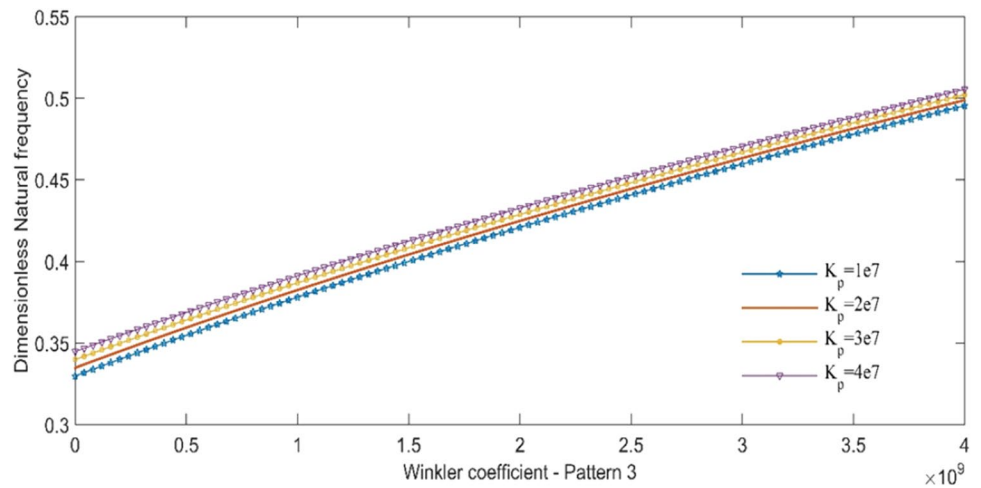


Fig. 7 Elastic foundation effects on frequency of GPLRC beam (pattern 4)

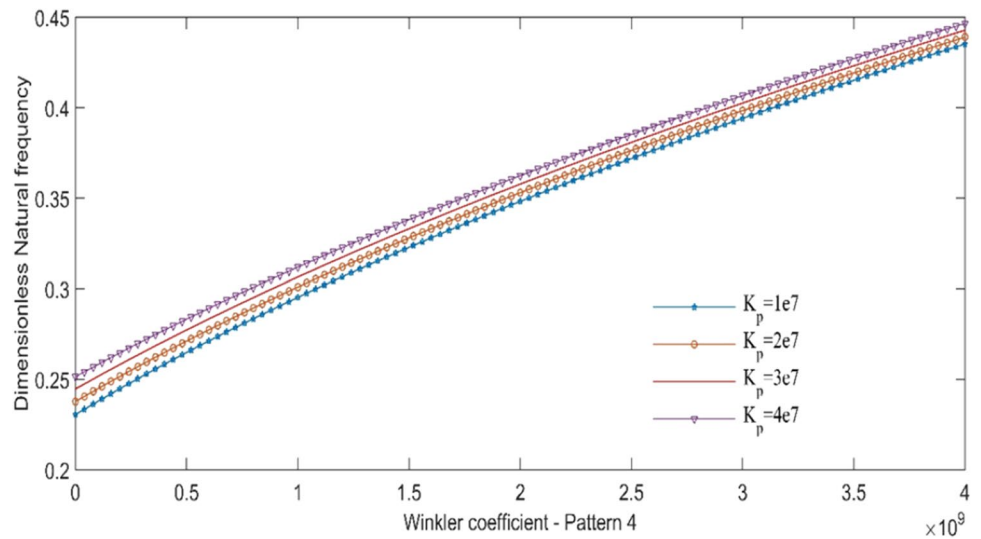
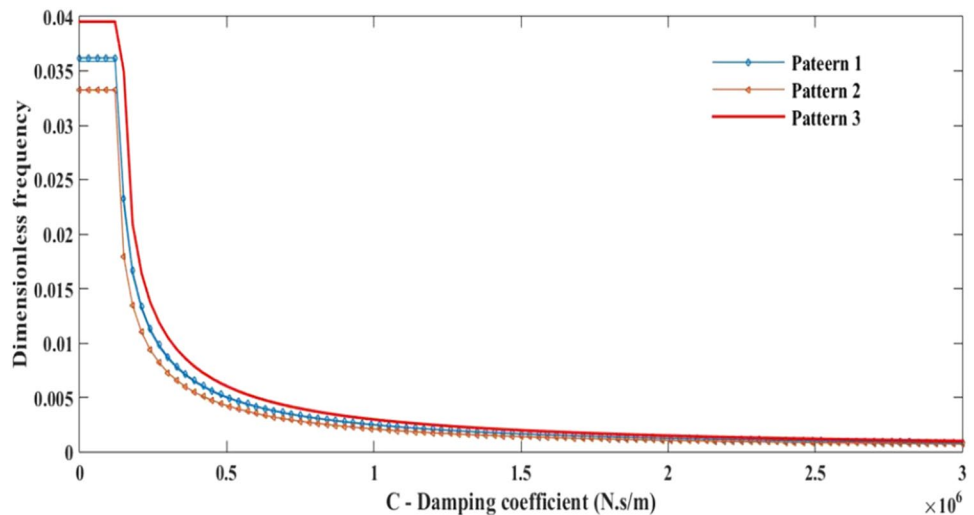


Table 2 Winkler and Pasternak coefficient effects on natural frequency of multi-layer GPLRC beam ($a/h = 10, \bar{\lambda} = 10^3 \omega$)

$\bar{\lambda}$	$K_p = 0$		$K_p = 25e5$		$K_p = 5e6$		$K_p = 75e5$	
	Pattern 1	Pattern 2	Pattern 1	Pattern 2	Pattern 1	Pattern 2	Pattern 1	Pattern 2
$K_w = 0$	0.6537	0.5741	0.7946	0.7305	0.914	0.8588	1.0195	0.9703
$K_w = 2e6$	0.6662	0.5883	0.8049	0.7417	0.923	0.8684	1.0276	0.9788
$K_w = 4e6$	0.6775	0.6022	0.8151	0.7528	0.9319	0.8779	1.0356	0.9872
$K_w = 6e6$	0.6906	0.6158	0.8252	0.7637	0.9407	0.8772	1.0436	0.9956
$K_w = 8e6$	0.7025	0.6921	0.8352	0.7744	0.9495	0.8965	1.0514	0.0039
$K_w = 10e6$	0.7141	0.6421	0.845	0.785	0.9581	0.9057	1.0593	0.0121

Fig. 8 Damper effects on dimensionless frequency parameter (λ) of GPLRC beam ($K_w = 100 \text{ N/m}, K_p = 100 \text{ N}$)



(middle layers included the most weight fraction of GPLs). In this table by varying numerical amount of Pasternak coefficient, it is clear that in constant Winkler coefficient, by increasing K_p , natural frequency is increased too. Comparing pattern 1 and 2 emphasized on bigger amount of frequency for pattern 1 than pattern 2 in the same amount of K_p .

6.3 Effects of damper on dimensionless frequency of GPLRC beam

Damper coefficient increasing is investigated in this part and effects of C_d on GPLRC beam vibrational behavior in constant elastic factors is shown in Fig. 8. By varying C_d to bigger amount, dimensionless frequency is constant at first but by leading to bigger amount of this coefficient, decreasing process in all four patterns is resulted. C_d as damper factor is varying from 0 to $3 \times 10^6 \text{ Ns/m}$.

Numerical results of dimensionless frequency of GPLRC beam in different amount of C_d is presented by Table 3 (GPL weight fraction amount is 0.12). Results is showed that by leading damper factor to bigger number, dimensionless frequency of the structure is showed decreasing process in all patterns.

Table 3 Dimensionless natural frequency parameter (λ) by varying damper coefficient and four GPLs distribution patterns ($K_p = 100 \text{ N}, K_w = 100 \text{ N/m}, g_{GPL} = 0.12$)

GPL pattern	Pure epoxy	Pattern 1	Pattern 2	Pattern 3	Pattern 4
$C_d = 0 \text{ Ns/m}$	0.0292	0.0362	0.0332	0.0395	0.0395
$C_d = 6e5 \text{ Ns/m}$	0.0027	0.0041	0.0035	0.0049	0.0049
$C_d = 12e5 \text{ Ns/m}$	0.0013	0.0020	0.0017	0.0024	0.0024
$C_d = 18e5 \text{ Ns/m}$	0.0009	0.0013	0.0011	0.0016	0.0016
$C_d = 24e5 \text{ Ns/m}$	0.0006	0.0010	0.0008	0.0012	0.0012
$C_d = 30e5 \text{ Ns/m}$	0.0005	0.0008	0.0006	0.0009	0.0009

7 Conclusions

1. Increasing damper coefficient resulted in smaller amount of dimensionless natural frequency in all four GPL distribution and pure epoxy (Table 3).
2. By varying C_d to bigger amount, dimensionless frequency is constant at first but by leading to bigger amount of this coefficient, decreasing process in all four patterns is resulted (Fig. 8).
3. In constant Winkler coefficient amount, by K_p increasing, the natural frequency is increased (Table 2).

4. By increasing the amount of K_w and K_p the natural frequency of GPLRC beam is increased too in all four patterns (Table 2).
5. By adding GPLs to the structure and studying the effects of Pasternak factor on vibration behavior of GPLRC beam, results is showed that dimensionless frequency of the structure is increased by Pasternak factor increasing (Figs. 3, 4, 5, 6, 7).
6. By varying numerical amount of Pasternak coefficient, it is clear that in constant Winkler coefficient, by K_p increment, natural frequency is increased too (Table 2).

Compliance with ethical standards

Conflict of interest The authors declared no potential conflicts of interest with respect to the research, authorship, and/or publication of this article.

References

1. Ansari R, Hasrati E, Shojaei MF, Gholami R, Shahabodini A (2015) Forced vibration analysis of functionally graded carbon nanotube-reinforced composite plates using a numerical strategy. *Phys E Low Dimens Syst Nanostruct* 69:294–305
2. Balandin AA, Ghosh S, Bao W, Calizo I, Teweldebrhan D, Miao F, Lau CN (2008) Superior thermal conductivity of single-layer graphene. *Nano Lett* 8(3):902–907
3. Baradaran S, Moghaddam E, Basirun WJ, Mehrali M, Sookhaskian M, Hamdi M, Moghaddam MN, Alias Y (2014) Mechanical properties and biomedical applications of a nanotube hydroxyapatite-reduced graphene oxide composite. *Carbon* 69:32–45
4. Barati MR, Zenkour AM (2017) Post-buckling analysis of refined shear deformable graphene platelet reinforced beams with porosities and geometrical imperfection. *Compos Struct* 181:194–202
5. Chandra Y, Chowdhury R, Scarpa F, Adhikari S, Sienz J, Arnold C, Murmu T, Bould D (2012) Vibration frequency of graphene based composites: a multiscale approach. *Mater Sci Eng B* 177(3):303–310
6. Chu NH, Feng C, Yang J, Kitipornchai S (2017) Finite element analysis on free vibration of polymer composite beams reinforced with graphene platelets. In: *Mechanics of structures and materials: advancements and challenges—proceedings of the 24th Australasian conference on the mechanics of structures and materials, ACMSM24 2016*. CRC Press, Balkem, pp. 1803–1808
7. Du X, Skachko I, Barker A, Andrei EY (2008) Approaching ballistic transport in suspended graphene. *Nat Nanotechnol* 3(8):491
8. Feng C, Kitipornchai S, Yang J (2017) Nonlinear free vibration of functionally graded polymer composite beams reinforced with graphene nanoplatelets (GPLs). *Eng Struct* 140:110–119
9. Feng C, Kitipornchai S, Yang J (2017) Nonlinear bending of polymer nanocomposite beams reinforced with non-uniformly distributed graphene platelets (GPLs). *Compos Part B Eng* 110:132–140
10. Gauvin F, Robert M (2015) Durability study of vinylester/silicate nanocomposites for civil engineering applications. *Polym Degrad Stab* 121:359–368
11. Huang X, Qi X, Boey F, Zhang H (2012) Graphene-based composites. *Chem Soc Rev* 41(2):666–686
12. Ji XY, Cao YP, Feng XQ (2010) Micromechanics prediction of the effective elastic moduli of graphene sheet-reinforced polymer nanocomposites. *Model Simul Mater Sci Eng* 18(4):045005
13. Ke LL, Yang J, Kitipornchai S (2013) Dynamic stability of functionally graded carbon nanotube-reinforced composite beams. *Mech Adv Mater Struct* 20(1):28–37
14. Ke LL, Yang J, Kitipornchai S (2010) Nonlinear free vibration of functionally graded carbon nanotube-reinforced composite beams. *Compos Struct* 92(3):676–683
15. King JA, Klimek DR, Miskioglu I, Odegard GM (2013) Mechanical properties of graphene nanoplatelet/epoxy composites. *J Appl Polym Sci* 128(6):4217–4223
16. Kitipornchai S, Chen D, Yang J (2017) Free vibration and elastic buckling of functionally graded porous beams reinforced by graphene platelets. *Mater Des* 116:656–665
17. Liu J, Yan H, Jiang K (2013) Mechanical properties of graphene platelet-reinforced alumina ceramic composites. *Ceram Int* 39(6):6215–6221
18. Montazeri A, Rafii-Tabar H (2011) Multiscale modeling of graphene-and nanotube-based reinforced polymer nanocomposites. *Phys Lett A* 375(45):4034–4040
19. Mortazavi B, Benzerara O, Meyer H, Bardon J, Ahzi S (2013) Combined molecular dynamics-finite element multiscale modeling of thermal conduction in graphene epoxy nanocomposites. *Carbon* 60:356–365
20. Potts JR, Dreyer DR, Bielawski CW, Ruoff RS (2011) Graphene-based polymer nanocomposites. *Polymer* 52(1):5–25
21. Rafiee M, Yang J, Kitipornchai S (2013) Large amplitude vibration of carbon nanotube reinforced functionally graded composite beams with piezoelectric layers. *Compos Struct* 96:716–725
22. Rafiee M, Yang J, Kitipornchai S (2013) Thermal bifurcation buckling of piezoelectric carbon nanotube reinforced composite beams. *Comput Math Appl* 66(7):1147–1160
23. Rafiee MA, Rafiee J, Srivastava I, Wang Z, Song H, Yu ZZ, Koratkar N (2010) Fracture and fatigue in graphene nanocomposites. *Small* 6(2):179–183
24. Rafiee MA, Rafiee J, Wang Z, Song H, Yu ZZ, Koratkar N (2009) Enhanced mechanical properties of nanocomposites at low graphene content. *ACS Nano* 3(12):3884–3890
25. Rafiee MA, Rafiee J, Yu ZZ, Koratkar N (2009) Buckling resistant graphene nanocomposites. *Appl Phys Lett* 95(22):223103
26. Shabanlou G, Hosseini SAA, Zamanian M (2017) Vibrations analysis of FG spinning beam using higher order shear deformation beam theory in thermal environment. *Appl Math Model* 56:325–341
27. Song M, Kitipornchai S, Yang J (2017) Free and forced vibrations of functionally graded polymer composite plates reinforced with graphene nanoplatelets. *Compos Struct* 159:579–588
28. Spanos KN, Georgantzinos SK, Anifantis NK (2015) Mechanical properties of graphene nanocomposites: a multiscale finite element prediction. *Compos Struct* 132:536–544
29. Wang Y, Yu J, Dai W, Song Y, Wang D, Zeng L, Jiang N (2015) Enhanced thermal and electrical properties of epoxy composites reinforced with graphene nanoplatelets. *Polym Compos* 36(3):556–565

30. Wei X, Lee C, Kysar JW, Hone J (2008) Measurement of the elastic properties and intrinsic strength of monolayer graphene. *Science* 321(5887):385–388
31. Wu H, Kitipornchai S, Yang J (2015) Free vibration and buckling analysis of sandwich beams with functionally graded carbon nanotube-reinforced composite face sheets. *Int J Struct Stab Dyn* 15(07):1540011

Publisher's Note Springer Nature remains neutral with regard to jurisdictional claims in published maps and institutional affiliations.